scribed above is the existence of non-Rayleigh, high-frequency surface modes in monatomic crystals. It may be possible to observe such modes (and other types of surface modes) with the scattering of light atoms.[7]

*Work supported by the U. S. Air Force Office of Scientific Research under Grant No. AF-AFOSR 1257-67.

[1]By "Rayleigh modes" we mean modes belonging to those branches which give true Rayleigh waves in the long-wavelength limit for an isotropic medium.

[2]The model is more realistic than those used in other studies of surface modes in monatomic crystals in that an atom interacts with all of its neighbors and the displacements of the atoms near the surface from their bulk positions are taken into account. Also, no simplifying assumptions about isotropy, decoupling of vibrations in different directions, etc., are made. The atoms are taken to interact through a Lennard-Jones 12-6 potential, but the form of the interatomic potential is not expected to have an important effect on the qualitative features of the frequency spectrum. The model crystals also have finite thicknesses, but one finds that this feature does not have an important effect on the surface modes for thicknesses of 10 layers or more (except to produce a splitting of the frequencies; see Ref. 6).

[3]The "band gaps" referred to here are gaps in the range of frequencies for a particular two-dimensional wave vector (q_x,q_y) rather than a gap in the range of frequencies for all q_x and q_y (i.e., a true band gap).

[4]The possibility of such modes has been recognized, of course. See T. E. Feuchtwang, Phys. Rev. 155, 731 (1967).

[5]R. E. Allen and F. W. de Wette, Phys. Rev. 179, 873 (1969).

[6]In a crystal with two surfaces, there are actually two surface modes of each kind which are mixtures of the degenerate pair of modes for the individual surfaces, with the degeneracy slightly broken by the finite thickness.

[7]N. Cabrera, V. Celli, and R. Manson, Phys. Rev. Letters 22, 346 (1969).

MAGNETOMORPHIC SIZE EFFECT IN TUNGSTEN

D. E. Soule and J. C. Abele
Douglas Advanced Research Laboratories, Huntington Beach, California 92647
(Received 25 August 1969)

The magnetomorphic size effect was found in tungsten single crystals. Analytic Fermi-surface models, one of which is calculated here from de Haas–van Alphen results, are analyzed to show that the observed electronic orbital bands originate on the hole octahedron in an inflection region for $\vec{H} \| \langle 100 \rangle$ and in an extended limiting point region for $\langle 111 \rangle$. Preliminary evidence also is discussed for limiting point orbits on the hole ellipsoids.

The Sondheimer magnetomorphic size effect[1] gives an insight into the dynamics of electrons in a magnetic field H by relating the observed oscillatory period ΔH to the average component of the orbital momentum $m_c^* \bar{v}_H$ in the direction of $\vec{H}$. This in turn gives the orbital-area derivative $R = (\frac{1}{2}\pi)\partial A/\partial k_H$ for the particular band of relevant electronic orbits. Definitive studies have been made on the metals Na,[2] Cd,[3] Ga,[4] and Al.[5] Fermi surfaces (FS) could generally be approximated by the nearly-free-electron band model, with an emphasis on elliptic limiting and extended limiting point orbits. Here we investigate the effect of several types of orbital bands in tungsten. Since this derivative type effect is sensitive to small perturbations in the FS shape, the approach is to formulate FS models directly from the de Haas-van Alphen (dHvA) data and then to relate the calculated R values to the observed magnitude and orientation behavior of ΔH to confirm the origin of relevant orbits.

We observed the magnetomorphic oscillations in the Hall effect and transverse magnetoresistance of thin single-crystal plates of tungsten. Oscillations were studied up to 19 kG at $T = 1.3$ to 4.2°K over a range of tilt angles θ from the sample normal $\vec{n}$, using $\{100\}$ and $\{110\}$ magnetic field rotation planes. The samples were bridge-shaped plates that were spark cut from a tungsten boule having a residual resistance ratio of $\simeq$42 000. They were then carefully polished to final thicknesses d ranging from 75 to 298 μ. Crystallographic orientations were kept to within 1-2°. Representative XY recorder traces for ρ_{11} and ρ_{12} taken on a $\{100\}$ sample with $d = 90.5 \pm 2$ μ are shown in Fig. 1 for several tilt angles in the $\{100\}$ rotation plane. As can be seen in the figure, the relative amplitude of the Hall resistivity oscillations far exceeds that of the magnetoresistivity. For example, at 15 kG,

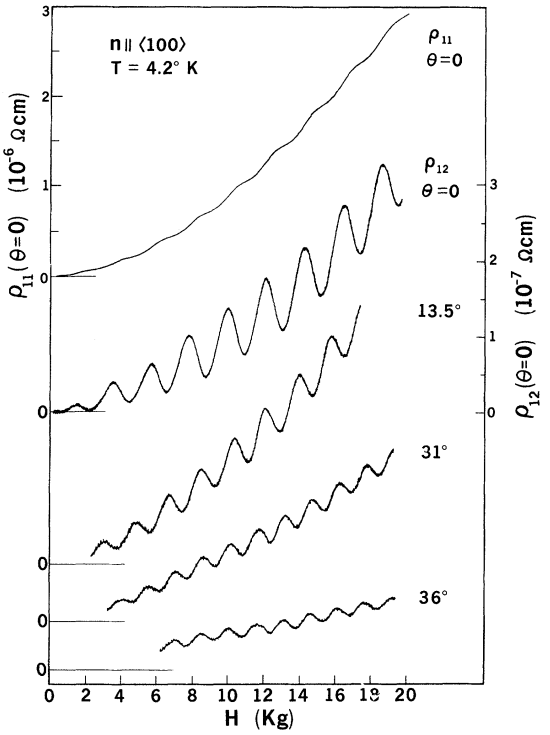

FIG. 1. Recorder traces of magnetomorphic oscillations in ρ_{11} and ρ_{12} at several tilt angles θ.

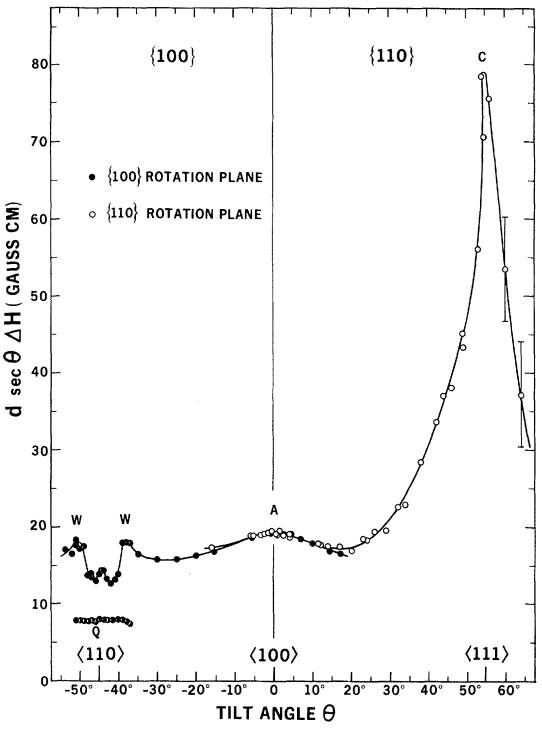

FIG. 2. Reduced Hall $\Delta\rho_{12}$ period vs θ on a $\{100\}$ sample for $\{100\}$ and $\{110\}$ H-rotation planes. The results of several separate runs are superimposed. The error brackets indicate the estimated error near $\langle 111\rangle$.

$\Delta\rho_{12}/\rho_{12}$ is 24%, while $\Delta\rho_{11}/\rho_{11}$ is only 1.9%. The decay in amplitude with θ is governed by the factor $\exp(-d\sec\theta/l_B)$, where l_B is the bulk mean-free path. Since no appreciable increase in the oscillatory amplitude was observed down to 1.3°K for these samples, they are considered to have been in the impurity scattering region throughout. These highly sinusoidal oscillations are strictly periodic in H over the whole H range. The periods observed for $\Delta\rho_{11}$ and $|\Delta\rho_{12}|$ agree to within 0.9% and the phase difference is 0.62π. Further θ dependence of the period will hereafter refer to that of $\Delta\rho_{12}$.

The behavior of the reduced oscillatory period $\Delta H_0 = d\Delta H \sec\theta$ vs θ, observed for the $\{110\}$ and $\{100\}$ H rotation planes, is shown in Fig. 2. The most striking feature is the steep rise to a sharp peak at $\langle 111\rangle$ from 19.4 to 79 G cm. Correspondingly, the oscillatory amplitude decreased smoothly with θ, suggesting a gradual rotation of a band of orbits on a single FS. A sharply defined "window" is seen between W's about the $\langle 110\rangle$ direction, where ΔH_0 drops to an average of 13.7 G cm. This region of lower amplitude reveals a second smaller $\Delta H_0 = 7.92$ G cm shown at Q. Since the above results were taken on a $\{100\}$ sample, there is a loss in accuracy in the $\langle 111\rangle$ and $\langle 110\rangle$ directions. The azimuthal crystallographic misorientation away from the magnetic-field rotation plane is about 1-2°. This alignment error does not significantly affect the accuracy of ΔH_0 in the $\langle 100\rangle$ direction, but at $\langle 111\rangle$, however, it can be a problem.

To interpret these results, we shall concentrate primarily on the orientation dependence of the oscillatory periods. The period ΔH is the interval in H during which an additional cyclotron orbit is traversed during an electron's helical transit across the crystal. The transit time is governed by $\bar{v}_H$, the average drift-velocity component along $\vec{H}$. The number of revolutions is

$$N = \omega d \sec\theta / 2\pi \bar{v}_H, \tag{1}$$

where ω is the cyclotron frequency. The reduced period is then

$$\Delta H_0 = (2\pi c/e) m_c^* \bar{v}_H = (hc/e)(\tfrac{1}{2}\pi)\partial A/\partial k_H = (hc/e)R. \tag{2}$$

The orbital-area derivative R can then be used to characterize the curvature R^{-2} of certain regions on the FS. In the limit of a spherical

FS, R approaches the radius of curvature.

The basic types of electronic orbit groups that can give rise to magnetomorphic oscillations are these: I. Limiting-point orbits, where a small group of orbits in the immediate neighborhood of the limiting point are involved, having velocities $\vec{v}_H \to \vec{v}_F$, the total Fermi velocity. II. Inflection band orbits, where the orbit group is located in an inflection region on the FS where R has an extremal value. III. Δk_H band orbits, where a larger group of orbits is located in a region of constant R of width Δk_H. I-III. Extended limiting-point orbits, where a larger orbit group is located in an extended region of constant R containing the limiting point, such as a paraboloidal FS.

The relative probability of observing a particular group of orbits depends primarily upon the number of electrons involved and the magnitude of ΔH_0 through the amplitude factor R^S, where S takes values of 7, 4, and 3 for orbit types I, II, and III, respectively.[4] It is clear that those groups with a large ΔH_0 will dominate the observed oscillations, as will be seen here for the hole octahedron.

The sharp peak at ⟨111⟩ shown in Fig. 2 strongly suggests a shallow curved {111} FS facet, as exists on the hole octahedron or on the octahedral body of the electron jack. In order to confirm the origin of this signal, we calculated R vs k_H from analytical FS models for the ⟨100⟩ and ⟨111⟩ $\vec{H}$ directions. The first of such models was determined by Girvan, Gold, and Phillips (GGP)[6] from a least-squares fit to their observed dHvA data. The particular FS's will be considered in ascending order of their potential relevance to the present measurement.

The hole ellipsoids located on the {110} Brillouin-zone faces have limiting points K (4 ellipsoids) and L (2 ellipsoids) for $\vec{H} \parallel \langle 100 \rangle$ as shown in Fig. 3. The calculated R's are linear in k_H with low values of -0.192 Å^{-1} at K and -0.0924 Å^{-1} at L. In addition, these would give low-amplitude signals and therefore are not observed in our {110} rotation-plane results.

GGP constructed a composite analytical model for the electron jack consisting of knobs, with a rounded square shape, joined smoothly to a rounded and slightly indented octahedral body.[7] Derivatives R were calculated for the knob using

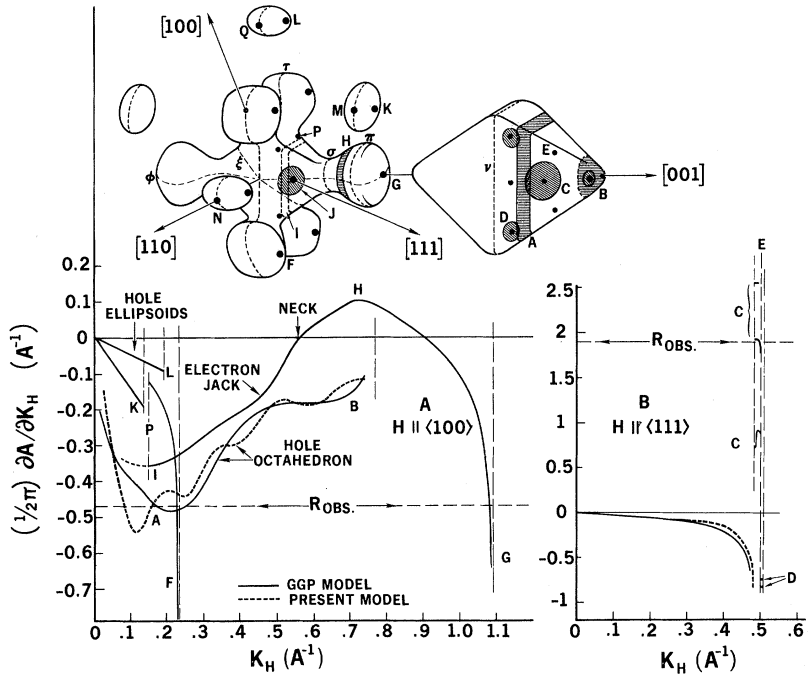

FIG. 3. Comparison of observed R_{obs} and orbital-area derivative vs k_H calculated from Fermi surface (FS) models. All tungsten FS's are represented for ⟨100⟩ in A, and the hole octahedron is shown for ⟨111⟩ in B. The vector k_H is measured from the center of each FS, and vertical dashed lines indicate limiting or saddle points. Relevant orbital bands are identified on the right halves of the FS's only. Greek letters identify the external dHvA orbits.

area slices to within 0.000 09 $Å^{-1}$ of the limiting point at F and to within 0.0002 $Å^{-1}$ of G, giving values of $>|-0.89\ Å^{-1}|$ and $>|-2.41\ Å^{-1}|$, respectively, —well away from the observed derivative R_{obs}. The exact shape at these limiting points depends critically on the accuracy of the dHvA fit. For example, the dHvA π-extremal orbit shown in Fig. 3 would be expected to give a good representation of the knob shape at F, whereas the τ or φ extremal orbits, encompassing the total jack surface, would give correspondingly poorer fits to the surface at G. An inflection region occurs at H with a derivative of about 0.10 $Å^{-1}$. At lower k_H, R decreases to a possible minimum of -0.357 $Å^{-1}$ at I, which almost coincides along k_H with the cutoff P at the juncture of the body and neck. Therefore, it is uncertain whether such an orbital band exists or is interrupted by the neck regions. Unfortunately, the surface on the jack is not well enough specified in this region, since the dHvA fit of the ζ orbit is doubtful.[6] In any case, the magnitude of the calculated R does not match R_{obs}. Also, a smooth transition of a single orbital band over the FS from $\langle 100\rangle$ to $\langle 111\rangle$ is not possible on the jack surface, thus ruling it out as a likely source.

The most probable FS is the hole octahedron, for which we have analyzed two different analytical FS models. The first is the three-parameter model of GGP fit by least squares to extremal areas from their dHvA data.[6] For the second model, we have applied the inversion scheme of Mueller,[8] assuming that the hole octahedron is centrally symmetric and has a single-valued radius vector, as justified by band calculations[9] and the accepted interpretation of the dHvA data of Sparlin and Marcus (SM)[10] and of GGP. Following Mueller and introducing cubic symmetry, we least-squares fit the dHvA data to the cross-sectional area expansion

$$A(\theta', \varphi') = \sum_{i,l} {}_i\beta_l\, {}_iK_l, \tag{3}$$

where ${}_iK_l = \sum_m {}_ia_{lm}c_{lm}$ are the cubic harmonics composed of the real spherical harmonics c_{lm}, using the coefficients ${}_ia_{lm}$ tabulated by Mueller and Priestley.[11] The experimental data we used are those of GGP and SM, which were standardized to the extremal $A_{\langle 111\rangle}$ value of 9.88×10^7 G, as measured by O'Sullivan and Schirber.[12] In order to minimize the fluctuation in the expansion, we performed a graphical smoothing of the data and took 69 equally spaced points in the $\{100\}$ and $\{110\}$ planes. Also, the expansion was extended to the $l = 16$ cubic harmonic. The average rms error in the area expansion is 0.16%, with a maximum deviation of 0.61%. Mueller's technique also yields the expansion for the radius-vector squared:

$$k^2(\theta', \varphi') = \sum_{i,l} {}_i\gamma_l\, {}_iK_l, \tag{4}$$

where ${}_i\gamma_l = {}_i\beta_l/\pi P_l(0)$ are the expansion coefficients in the θ' and φ' spherical coordinate system, $P_l(0)$ being Legendre polynomials. The resulting principal radius vectors for this model are $k_{\langle 100\rangle} = 0.765\ Å^{-1}$, $k_{\langle 110\rangle} = 0.592\ Å^{-1}$, and $k_{\langle 111\rangle} = 0.483 \pm 0.006\ Å^{-1}$. For the latter value, the uncertainty is due to local fluctuations in the FS model believed to be caused by the limited number of harmonics used, and by the availability of only the $\{100\}$- and $\{110\}$-plane dHvA data.

The calculated R-vs-k_H curves at $\langle 100\rangle$ are shown for these two hole octahedron models in Fig. 3(a). A dominant minimum occurs for both models at A, with values of $-0.483\ Å^{-1}$ for the GGP model and $-0.491 \pm 0.049\ Å^{-1}$ for the present model, where the fluctuations are again believed to be due to the harmonic and dHvA-data limits. The absolute values of these R's are in good agreement with $R_{obs} = 0.470 \pm 0.009\ Å^{-1}$. As a result, the primary observed oscillatory term at $\langle 100\rangle$ is believed due to a type-II inflection band of orbits as located at A on the FS in the figure. It is possible that another band of type I-III may exist at the octahedron vertex at B. Its uncertainty is due to the fact that the vertex constitutes a small fraction of the extremal area of the dHvA ν orbit.

In the $\langle 111\rangle$ direction where ΔH_0 goes through such a sharp peak, a quantitative comparison is even more critically dependent on the exact FS-model shape. The results for both models show in Fig. 3(b) that a large $|R|$ occurs only on the slightly concave $\langle 111\rangle$ face of the octahedron at C. Here is where the GGP model, giving 0.826 $Å^{-1}$, differs from the present model, giving 1.93-2.56 $Å^{-1}$. Each shows an approximate paraboloidal-shaped surface producing a type I-III orbital band. Consequently, there is also substantial agreement at $\{111\}$ for the hole octahedron between the present FS model and $R_{obs} = 1.91 \pm 0.20\ Å^{-1}$, especially since the crystal's azimuthal misorientation discussed above tends to make this value the lower limit. As a result, it is believed that the actual $\{111\}$ face of the hole octahedron is somewhat flatter than the GGP model proposes. The divergence in R between the two FS models, both fitting the same

dHvA data, illustrates a situation where the dHvA extremal area per se is less sensitive. And further, the radio-frequency size-effect measurement of Walsh et al.,[13] that evidently gives the outer ⟨111⟩ caliper, is also less sensitive to the degree of indenting of this {111} face. The magnetomorphic effect, therefore, can be helpful in resolving this small perturbation in the FS shape. Additional limiting points exist on the trigonal protuberances at D on the {111} face. In both models these are approximately paraboloidal, yielding type I-III orbital bands with values of -0.727 and -0.826 Å^{-1} for the GGP and present models, respectively. A final point on the ⟨111⟩ results is that the GGP model for the electron-jack body would predict a flatter {111} face and therefore a large $R \simeq 7$ Å^{-1}.

A detailed behavior in the ⟨110⟩ direction has not been fully analyzed as yet. The occurrence of the "window" may be caused by the orbital band having to pass over two octahedron vertices in the transition between ⟨100⟩ and ⟨110⟩, instead of over one vertex as is the case in the ⟨110⟩ rotation plane. Of main interest here is the lowest period between W's with $R_{obs} = 0.192$ Å^{-1}. This term[14] is tentatively identified as being due to limiting points on the hole ellipsoids, based on the magnitude of R and on its constancy with θ. There are four ellipsoids having limiting points at M giving an $R = -0.128$ Å^{-1}, one ellipsoid with an N point giving -0.169 Å^{-1}, and one with a Q point giving -0.223 Å^{-1}. Weighting factors due to the number of ellipsoids and the amplitude factor R^S are 0.048, 0.11, and 1.0, respectively, showing the strong contribution of the Q limiting-point signal. This identification is being investigated further.

A final note concerns the internal crystal thickness d^*, effective for electron scattering due to the local surface roughness, nonparallelism of surfaces, and depth of the deformed layers. An indication of Δd, where $d = d^* + 2\Delta d$, can be obtained from the quantitative agreement between the calculated R and R_{obs} for the orbital band A on the hole octahedron. This gives $\Delta d \simeq 1.5\mu$ per surface. Alternatively, from the standpoint of dispersion of oscillatory signals due to Δd, the dropoff of the oscillatory amplitude at high H is significant at the ninth oscillation (~23%) giving a comparable $\Delta d < 2.5\ \mu$ per surface.

It is a pleasure to thank K. M. Eicher for his able assistance in the experiment, W. M. Walsh, Jr., for his illuminating comments on the rf size-effect measurement, and D. M. Sparlin for kindly sending his dHvA data.

[1]E. H. Sondheimer, Phys. Rev. 80, 401 (1950), and Advan. Phys. 1, 1 (1952).

[2]J. Babiskin and P. G. Siebenmann, Phys. Rev. 107, 1249 (1957).

[3]N. H. Zebouni, R. E. Hamburg, and H. J. Mackey, Phys. Rev. Letters 11, 260 (1963); C. G. Grenier, K. R. Efferson, and J. M. Reynolds, Phys. Rev. 143, 406 (1966).

[4]J. A. Munarin, J. A. Marcus, and P. E. Bloomfield, Phys. Rev. 172, 718 (1968).

[5]K. Forsvoll and I. Holwech, Phil. Mag. 9, 435 (1964); T. Alstadheim and R. Risnes, Phil. Mag. 18, 885 (1968).

[6]R. F. Girvan, A. V. Gold, and R. A. Phillips, J. Phys. Chem. Solids 29, 1485 (1968).

[7]See Ref. 6, Eqs. (3)-(10).

[8]F. M. Mueller, Phys. Rev. 148, 636 (1966).

[9]See, for example, W. M. Lomer, Proc. Phys. Soc. (London) 84, 327 (1964); L. F. Mattheiss, Phys. Rev. 139, A1893 (1965); T. L. Loucks, Phys. Rev. 143, 506 (1966).

[10]D. M. Sparlin and J. A. Marcus, Phys. Rev. 144, 484 (1966).

[11]F. M. Mueller and M. G. Priestley, Phys. Rev. 148, 638 (1966).

[12]W. J. O'Sullivan and J. E. Schirber, Cryogen. 7, 118 (1967).

[13]W. M. Walsh, Jr., C. C. Grimes, G. Adams, and L. W. Rupp, Jr., in Proceedings of the Ninth International Conference on Low Temperature Physics, Columbus, Ohio, 1964, edited by J. G. Daunt (Plenum Press, Inc., New York, 1965), p. 765.

[14]It may correspond to the smaller of two periods (0.200 Å^{-1}) reported from rf size-effect measurements at ⟨110⟩ by R. F. Girvan and P. C. Canepa, Bull. Am. Phys. Soc. 14, 29 (1969).